Far infrared near normal specular reflectivity of $Ni_x(SiO_2)_{1-x}$, (x= 1.0, 0.84, 0.75, 0.61, 0.54, 0.28) granular films

Néstor E. Massa [a,1], Juliano C. Denardin [b,2], Leandro M. Socolovsky [c,3] Marcelo Knobel[d,4], Fernando P. de la Cruz,[a,5] and XiXiang Zhang [e,6]

[a] Laboratorio Nacional de Investigación y Servicios en Espectroscopía Optica- CEQUINOR, Universidad Nacional de La Plata, C.C. 962 , 1900 La Plata, Argentina,
[b] Departamento de Física, Universidad de Santiago de Chile, Av. Ecuador 3493, Santiago, . Chile,
[c.] Instituto de Tecnologías y Ciencias de la Ingeniería,Universidad de Buenos Aires, Av.Paseo Colón 850, Buenos Aires, Argentina
[d.] Instituto de Física, "Gleb Wataghin", Universidade Estadual de Campinas, 13083-970, Campinas, SP, Brazil,
[e.] Physics Department and Institute of Nanoscience and Technology, Hong Kong, University of Science and Technology, Clear Water Bay, Kowloon, Hong Kong, China.

[1]neemmassa@gmail.com, [2]jdenardin@usach.cl,[3] leandrosocolovsky@gmail.com, [4]knobel@ifi.unicamp.br, [5]fpdelacruz@yahoo.com.ar, [6]phxxz@ust.hk

One of the current issues at the basis of the understanding of novel materials is the degree of the role played by spatial inhomogeneities due to subtle phase separations. To clarify this picture here we compare the plain glass network response of transition metal granular films with different metal fractions against what it is known for conducting oxides Films for $Ni_x(SiO_2)_{1-x}$, x= 1.0, 0.84,0.75, 0.61,0.54, 0.28, were studied by temperature dependent far infrared measurements. While for pure Ni the spectrum shows a flat high reflectivity, those for x ~0.84 and ~0.75 have a Drude component, vibrational modes mostly carrier screened, and a long tail that extents toward near infrared. This is associated with hopping electron conductivity and strong electron-phonon interactions. The relative reduction of the number of carriers in $Ni_{0.75}(SiO_2)_{0.25}$ allows less screened phonon bands on the top of a continuum and a wide and overdamped oscillator at mid-infrared frequencies. $Ni_{0.54}(SiO_2)_{0.46}$ and $Ni_{0.28}(SiO_2)_{0.72}$ have well defined vibrational bands and a sharp threshold at ~1450 cm^{-1}. It is most remarkable a distinctive resonant peak at ~1250 cm^{-1} found for ***p***-polarized angle dependent specular reflectivity. It originates in an electron cloud traced to electrons that are not able to overcome the metal-dielectric interface that, beating against the positive background, generates the electric dipole. Overall, we conclude that the spectra are analogous to those regularly found in conducting oxides where with a suitable percolating network polarons are formed.

Keywords: A: disordered systems; A. oxide materials; C: electron-phonon interactions, C: optical properties, D: light absorption and reflection

Granular films provide grounds to expand the understanding on the carrier dynamics in heterogeneous systems, a subject that it is concomitant to a plethora of compounds and, in particular, to oxides. Here we explore, with tools regularly used in infrared spectroscopy, the optical conductivity of films made of metallic nanoobjects embedded in a SiO_2 insulating matrix. Transition metal 550 nm thick granular films $Ni_x(SiO_2)_{1-x}$, (x= 1.0, 0.84, 0.75, 0.61, 0.54, 0.28) were prepared by magnetron cosputtering being the Ni and SiO_2 deposited simultaneously on rotating glass and kapton substrates. Energy dispersive X-ray spectroscopy yielded ~7% of uncertainty for a film metal fraction. All our samples have been characterized by transmission electron microscopy (TEM) and with small (SAXS) and wide angle (WAXS)

X-ray scattering [1]. We conclude that the sputtering method generates amorphous structures, particles, and a variety of granular systems where, regardless the metal transition volume fraction, there is a ~29% of truly nanoparticles.[2]

Infrared spectroscopy between 30 cm^{-1} and 11000 cm^{-1} (wavelength ~1000 μ to ~2 μ , i.e., our metal nanoaggregates may be thought as "artificial metal atoms") were measured in a FT-IR Bruker 113v and a FT-IR Bruker 66 with 2 cm^{-1} (FIR) and with 6 cm^{-1} (MIR) resolution with the sample mounted in the cold finger of an Oxford DN 1754 cryostat. A gold mirror was used as 100 % reference. Polarized angle dependent measurements have been done using a Spectra Tech Series 500 specular reflectance accessory with a polarizer made of gold wire grid on a KRS-5 substrate.

We estimate phonon frequencies with a classical simulation of the dielectric function with damped Lorentzian oscillators adding, if required by the data, one term for the Drude plasma.[3] Its complete expression is given by

$$\varepsilon(\omega) = \varepsilon_\infty \prod_j \left[\frac{\omega_{jLO}{}^2 - \omega^2 + i\gamma_{jLO}\omega}{\omega_{jTO}{}^2 - \omega^2 + i\gamma_{jTO}\omega} \right] - \varepsilon_\infty \frac{\left[\omega_p{}^2 + i(\gamma_p - \gamma_0)\omega\right]}{\left[\omega(\omega - i\gamma_0)\right]}, \qquad (1)$$

where ε_∞ is the high-frequency dielectric function; ω_{jLO} and ω_{jTO} are the longitudinal and transverse jth optical frequencies with damping constants γ_{jLO} and γ_{jTO} respectively. The second term represents the Drude contribution where ω_p is the plasma frequency, γ_p its damping and γ_o is understood as a phenomenological damping introduced by the lattice drag. Considering that

$$\omega^2_p = 4\pi e^2 N / m^*, \qquad (2)$$

one can estimate an effective carrier concentration $N^*=Nm_0/m^*$ (m_0 and m^* are the free- and effective electron mass; N and N* are the number and the effective number of carriers, respectively).

Here we selected films with Ni metal fractions from the metallic to the insulating regime implying nanoaggregate spacing ranging from 3.8 nm (insulating) to 2.5 nm (metallic) Figure 1 shows the change in reflectivity as we decrease the metal fraction. As expected for pure sputtered Ni on a SiO_2 glass substrate we obtain a featureless high reflectivity spectra barely delineating the glass vibrational modes (likely due to film defects allowing substrate detection). At lower reflectivity , due to less carriers , the same behavior is observed for $Ni_{0.84}(SiO_2)_{0.16}$ As we still reduce further the transition metal fraction the number of carriers in $Ni_{0.75}(SiO_2)_{0.25}$ are not enough to completely screen vibrational bands. It also insinuates a bump at ~1400 cm^{-1} that it is characteristic of electron promotion in an hybridized Transition Metal3d--O2p environment. Then we would expect starting at about this metal fraction to have clear evidence of localized and itinerant carrier coexistence, and the formation of

polarons due to the strong interaction between charge carriers and the ions. $Ni_{0.54}(SiO_2)_{0.46}$ is near the threshold where the insulating and transition metal fractions are such that anomalous enhancements, in the contributions to the Hall resistivity and magnetoresistive measurements, are found. The film vibrational bands are well defined but since not all the conducting paths are truncated they appear, being infrared an additive technique, overlapped with an overdamped carrier continuum .This almost disappears in insulating $Ni_{0.28}(SiO_2)_{0.72}$
Figure 2 shows a detailed picture of constituents common to all our samples. As it is shown in the inset (figure 2) the complete infrared reflectivity of $Ni_{0.84}(SiO_2)_{0.16}$ and $Ni_{0.75}(SiO_2)_{0.25}$ in addition to screened phonon profiles has a Drude term centered at zero frequency similar to the known for highly correlated carriers in oxides The tail extending to higher energies is associated to photon excited carrier hopping accompanied by multiphonon processes in a strong electron-phonon environment. Our fits yield a plasma frequency at ~1.47 eV and ~1.0 eV from which, one may deduce ~10^{21} and ~10^{17} effective number of carriers respectively (these values must be thought as ballpark figures because the electron effective charge and mass are not yet reported in the literature). It is to note that in order to obtain an excellent fit to the experimental data it is necessary to introduce a highly overdamped oscillator at mid-infrared frequencies. We interpret this as the profile of convoluted states due to localized self-trapped photoexcited charges coexisting with freer hopping electrons and producing electronic transitions to mid-gap empty defect glass states.

To visualize the effect of localization and electron-phonon interactions, we analyzed the real part of experimental optical conductivity, $\sigma_1 = (\omega/4\pi)\varepsilon_2$ (ε_2 is the imaginary part of the dielectric function), with the current polaron models. Although this ought to be considered a mere preliminary approximation, since the film glass topology has not yet been addressed, we found that a fit using the small polaron formulation is useful to individualize the vibrational groups involved in the conductivity process. Thus, we use for every contributing vibrational band the theoretical expression by Reik and Heese at finite temperatures, $\sigma_1(\omega,\beta)$,[4] given by

$$\sigma_1(\omega,\beta) = \sigma_{DC}\frac{sinh\left(\frac{1}{2}\hbar\omega\beta\right)\exp\left[-\omega^2\tau^2 r(\omega)\right]}{\frac{1}{2}\hbar\omega\beta\left[1+(\omega\tau\Delta)^2\right]^{1/4}} \quad , (3)$$

$$r(\omega) = \left(\frac{2}{\omega\tau\Delta}\right)\ln\left\{\omega\tau\Delta+\left[1+(\omega\tau\Delta)^2\right]^{1/2}\right\} - \left[\frac{2}{(\omega\tau\Delta)^2}\right]\left\{\left[1+(\omega\tau\Delta)^2\right]^{1/2}-1\right\} \quad , (4)$$

with $\Delta = 2\varpi\tau$ and the relaxation time $\tau^2 = \frac{\left[sinh\left(\frac{1}{2}\hbar\varpi\beta\right)\right]}{2\varpi^2\eta}$. (5)

$\sigma_1(\omega,\beta)$, $\beta=1/kT$, is basically dependent on three parameters: $\sigma_{DC} = \sigma(0,\beta)$, the electrical conductivity (the fits yield an intermediate value of the one found with the conventional DC four points probe); the frequency ϖj, fixed by our measurements, corresponds to the average between the transverse and the longitudinal optical mode jth vibrational band, and η_j, being the only truly free parameter, characterizes the strength of the electron-phonon interaction for that mode.

Our results (figure 2 and Table I) show that by allowing independent uncorrelated contributions an excellent fit to the experimental data is achieved using eq.(3) leading to ϖ´s very close to the experimental main frequencies found by reflectivity. In particular, the vibrational group at ~948 cm^{-1}, i.e., glass stretching modes, and its overtone have distinctive contributions to the optical conductivity having the η's on the weaker interaction side.[4] On the other hand, the temperature behavior of the electron plasma in the films is as in most the oxides. As it is shown in figure 3a as the sample is cooled the scatter centers are reduced and the reflectivity due to carriers increases accordingly at the lowest frequencies. Figure 3 (b) shows the vibrational temperature dependent modes for a semiconducting film where the phonons appear on the top of a overdamped carrier continuum. As it was already pointed out above when we reduce the nanoparticles number it also implies a decrease in the number of carriers then allowing vibrational bands centered at ~480 cm^{-1} (bending) and ~980 cm^{-1} (stretching) be visible. We found that in addition of band profiles suggesting disordered induced broadening there is a new feature located at the minimum reflectivity, near the highest longitudinal mode (LO) frequency (~1210 cm^{-1}). Rising as a sharper localization edge at ~1450 cm^{-1} denotes strong electron-phonon interaction. This is of the same nature as those reported earlier, for example, for $NdNiO_3$ [5] Later verified in transport measurements by isotopic replacement,[6] that edge denotes the promotion of localized electrons to a lowest continuum. Best seen in our most insulating samples where localization is dominant and where most of conducting paths are truncated it also harbors a remarkable pure longitudinal excitation. To explore its nature we have used oblique reflectivity. This technique has been regularly used for detecting longitudinal optical modes, lattice vibrations perpendicular to a film surface, in transmission mode. [7] Radiation polarized perpendicular to the plane defined by the incident radiation and the normal to the film surface, transverse magnetic (TM) ***p***-polarized has a wave vector with components parallel and perpendicular to the film surface. Thus, extra bands not seen in transverse electric ***s***-polarization will appear. Almeida [8] showed that glass-SiO_2 sustains clear TO-LO splits for the main vibrational bands and that increasing the angle of incidence the overall band weigh shifts to higher frequencies peaking as expected at longitudinal modes. When this principle is applied to our samples a resonant band appears and becomes stronger with increasing angle being at ~70 º the dominant

feature. Shown in figure 4, the purely longitudinal character is emphasized by the detection for ***s***-polarization of a very strong antiresonance and that at higher angles merges with the vibrational longitudinal mode (figure 4 b). Ahn et al found that the new band is explained by noting that the tangential to the films component of the incident field has a null condition. [9] When this is fulfilled the normal component induces a collective electron oscillation as a localized nanoplasma in the metallic nanostructure. Then, the collective electron oscillation may be traced to electrons that are not able to overcome the metal-dielectric interface at the transition metal nanoparticles. Being localized, it pairs with the positive ion background to yield a strong infrared active electric dipole.

Concluding , we have discussed the infrared response of cosputtered granular films made of Ni and SiO_2 in different volume fractions. From metal oxide to insulating the reflectivity is dominated by electron hopping conductivity, strong electron –phonon interactions, polaron formation, and in the most insulating samples, by a remarkable resonance associated to a nanoplasma excitation. Overall, we conclude that the spectra are analogous to those regularly found in conducting oxides where with a suitable percolating network polarons are formed.[10]

References.

[1] J.C.Denardin, Ph.D thesis, Instituto de Física, Universidade Estadual de Campinas, Campinas, SP, Brazil.

[2] L. M. Socolovsky, C. L. P. Oliveria, J. C. Denardin, M. Knobel, and I. L. Torriani, Phys. Rev. B **72**, (2005) 184423-184428.

[3] N. E. Massa, H. Falcón, H. Salva, and R. E. Carbonio, Phys. Rev B **56** (1997) 10178-10191.

[4] . H. G. Reik, in *Polarons in Ionic Crystals and Polar Semiconductors*, edited by J. Devreese (North-Holland, Amsterdam), 1972. Also, H. G. Reik and D. Heese, J. Phys. Chem. Solids **28** (1967) 581-596.

[5] N. E. Massa, J. A. Alonso, M. J. Martínez-Lope, and I. Rasines. Phys. Rev. B. **56** (1997) 986-989.

[6] M. Medarde, P. Lacorre, K. Conder, F. Fauth, and A. Furrer. Phys. Rev. Lett. **80** (1998) 2397-2400

[7] D. W. Berreman, Phys. Rev. **130**, (1963) 2193-2198

[8] R. M. Almeida, Phys. Rev. B **45** (1992) 161-170.

[9] J. S. Ahn, H. S. Choi and T. W. Noh, Phys. Rev. **53**, (1996) 10310-10316.

[10] P. Calvani, O*ptical Properties of Polarons*, in La Rivista del Nuovo Cimento, **24**, (2001) 1-72.

Figure Captions

Figure 1 .*(WEB color)* Infrared reflectivity for $Ni_x(SiO_2)_{1-x}$ at 300 K as a function of the transition metal volume fraction.
Figure 2.*(WEB color)* The real part of the optical conductivity of $Ni_{0.84}(SiO_2)_{0.16}$ at 300 K. Full line upper trace is the optical conductivity drew from the measured reflectivity. The superposing dots are estimates using the small polaron approach. Individual gaussians correspond to different phonon contributions. Inset: Infrared reflectivity at 300 K for $Ni_{0.84}(SiO_2)_{0.16}$ and $Ni_{0.75}(SiO_2)_{0.25}$ showing the mid-infrared anomaly (circle: fit, line: data).
Figure 3 .*(WEB color)* Temperature dependent far infrared reflectivity for (a) $Ni_{0.75}(SiO_2)_{0.25}$; (b) $Ni_{0.54}(SiO_2)_{0.46}$
Figure 4 .*(WEB color)* 50º and 70º oblique incident $Ni_{0.28}(SiO_2)_{0.72}$ S- and P- reflectivity near the infrared nanoplasma resonant frequency at 300 K.

Table I

Parameters of the small polaron theory fit for the optical conductivity of $Ni_{0.84}(SiO_2)_{0.16}$ Note that vibrational frequencies are in agreement with the granular film IR experimental bands (in brakets) and that the conductivity tail (figure 2) is dominated by the overtone of the highest vibrational band at 974 cm^{-1}. The fit resistivity, ρ_{DC}, is also included.

ρ_{DC} (ohm-cm)	η_1	ϖ_{ph1} (cm^{-1})	η_2	ϖ_{ph2} (cm^{-1})	η_3	ϖ_{ph3} (cm^{-1})	η_4	ϖ_{ph4} (cm^{-1})	η_5	ϖ_{ph5} (cm^{-1})
0.00181	5.10	280.	2.26	380 (440)	4.30	647 (670)	4.85	948 (974)	6.29	1786

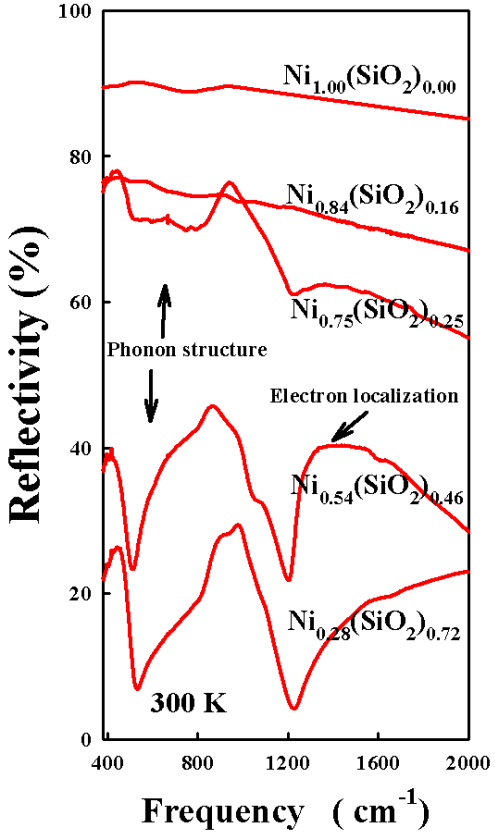

Figure 1
Massa et al

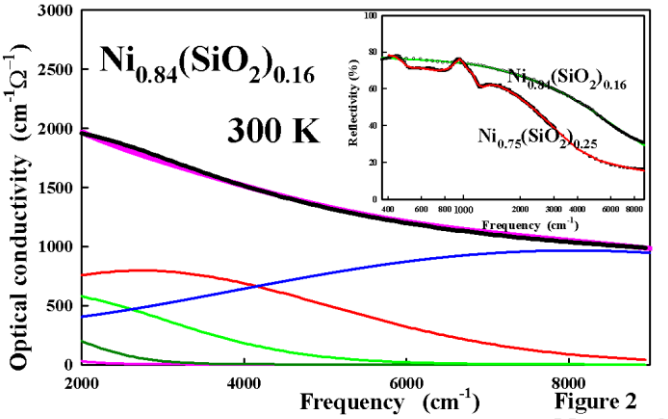

Figure 2
Massa et al

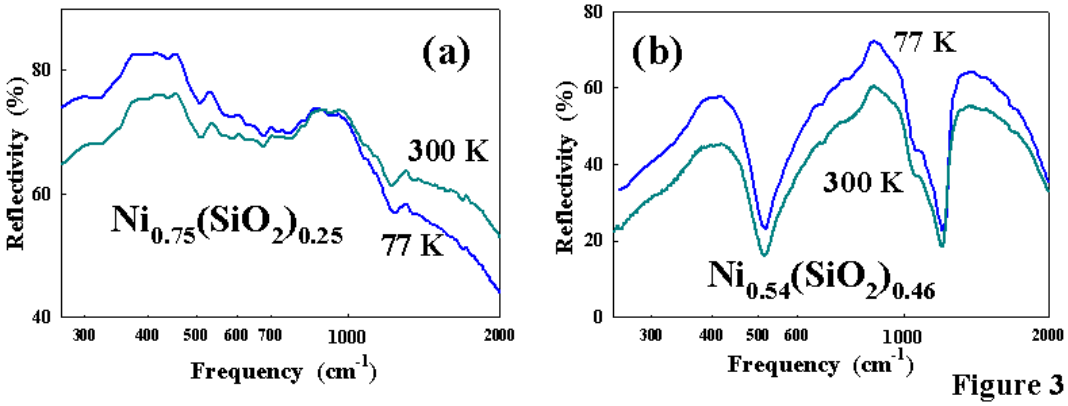

Figure 3
Massa et al

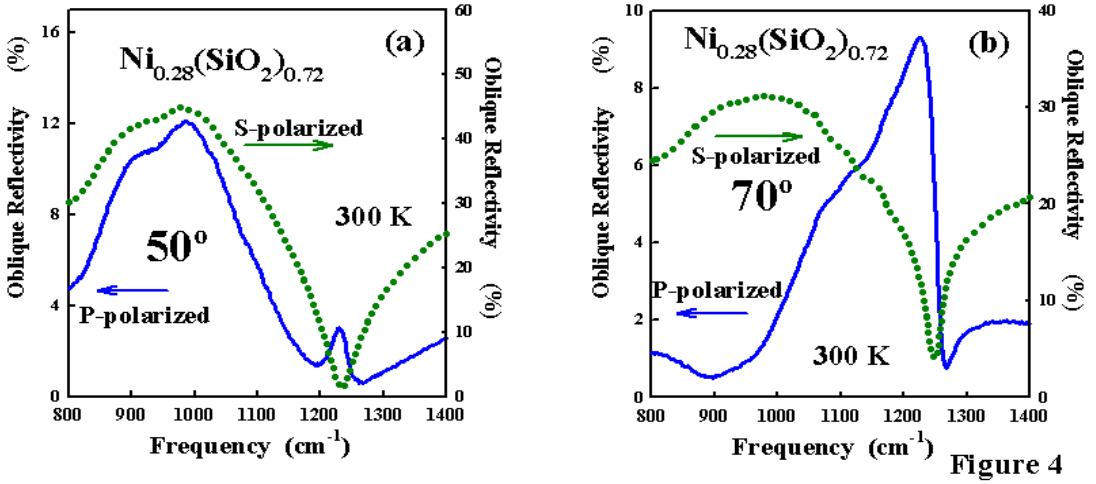

Figure 4
Massa et al

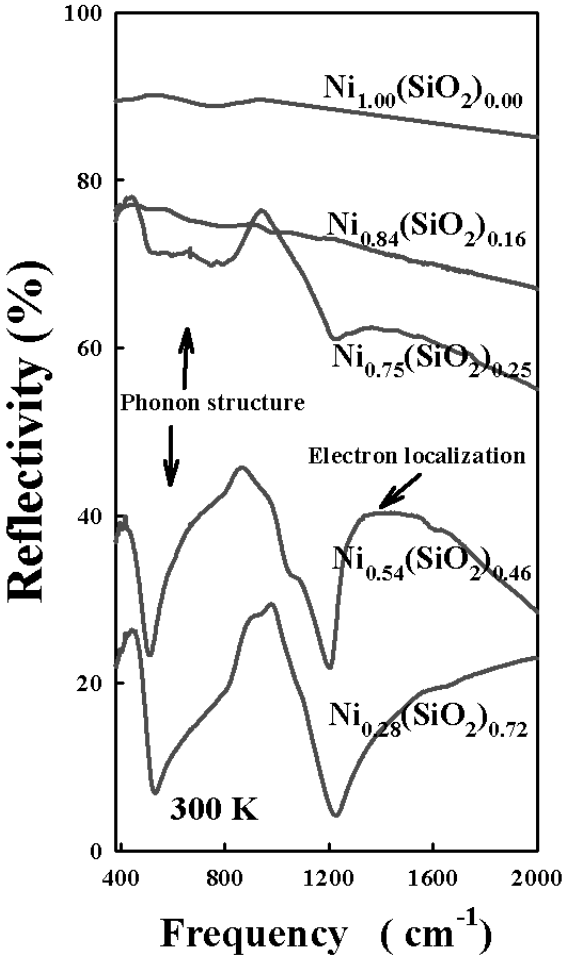

Figure 1
Massa et al

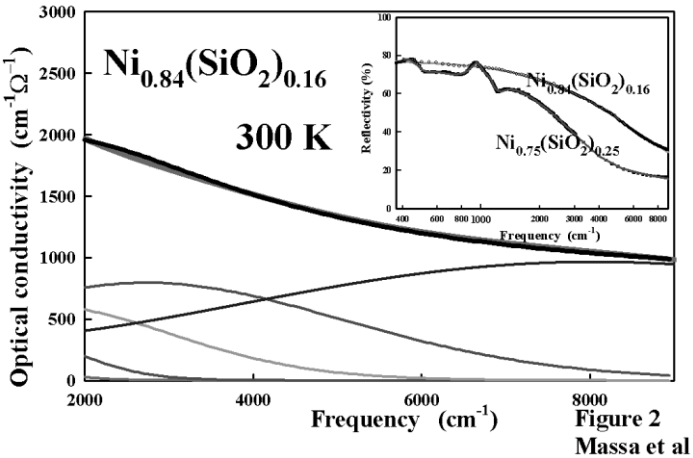

Figure 2
Massa et al

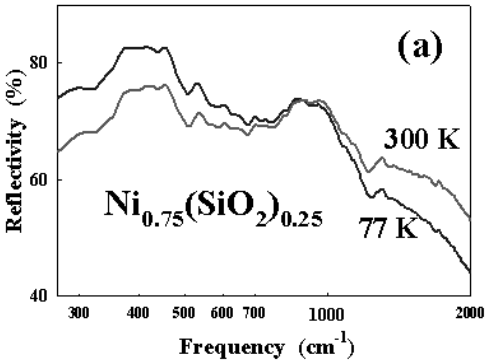

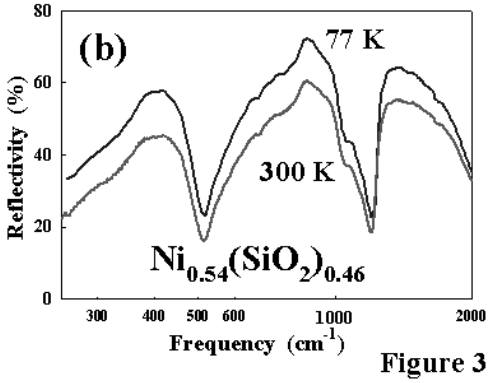

Figure 3
Massa et al

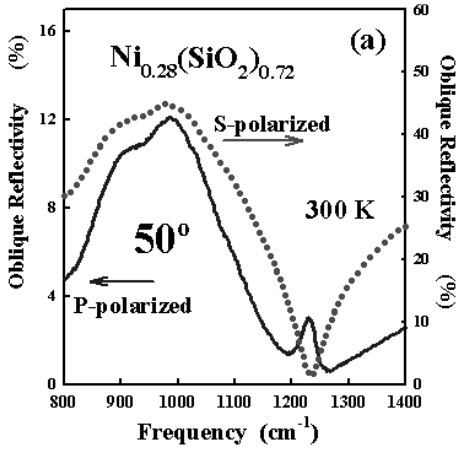

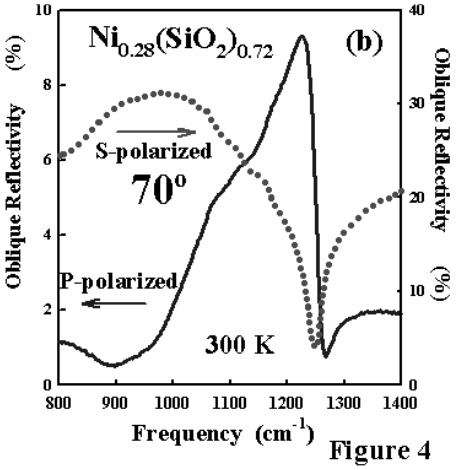

Figure 4
Massa et al